Application of ANN to Predict Liquefaction Potential

Vijay Kumar[1*], Kumar Venkatesh[2], R. P. Tiwari[3], Yeetendra Kumar[4]
[1,4]Research scholar, [2]Assistant Professor and [3]Professor.
Civil Engineering Department, Motilal Nehru National Institute of Technology, Allahabad, India Pin-211004.
Civil Engineering Department, Motilal Nehru National Institute of Technology, Allahabad, India, Pin-211004.

Abstract:
This study refers to the prediction of liquefaction potential of alluvial soil by artificial neural network models. To meet the objective 160 data sets from field and laboratory tests were collected for the development of ANN models. Initially these data sets were used to determine liquefaction parameters like cyclic resistance ratio and cyclic stress ratio by Idriss and Boulanger method to identify the liquefaction prone areas. Artificial neural network models were trained with six input vectors by optimum numbers of hidden layers, epoch and suitable transfer functions. Out of 160 data sets, 133 data sets were used for development of models and 27 datasets were used for validating the models. The predicted values of liquefaction potential by artificial neural networks models have been compared with Idriss and Boulanger method, which exhibits that trained artificial neural networks models are capable of predicting soils liquefaction potential adequately.

Keywords: Artificial Neural Network, Cyclic Resistance Ratio, Cyclic Stress Ratio, Idriss and Boulanger method, Liquefaction Potential.

1. Introduction:

Earthquake is kind of natural disaster, which occurs every year in the world. Engineers establish that soil comprising large amount of plastic fines has capability of liquefaction. Soil liquefaction is generally occurs in sand, silty sand and sandy silt soil [1]. Following conditions are required for liquefaction to occur:

- The soils must be submerged below the water table.
- The soil must be loose/soft to moderately dense/stiff.
- The ground shaking must be intense
- The duration of ground shaking must be sufficient for the soils to lose their shearing resistance.

Liquefaction resistance of plastic soil due to earthquake causes seriously destroying of structures like buildings, bridges, highways etc. Soil grains are complex set of particles of different size, shapes and gradations. Ground motion during earthquake is influenced by and affects properties of ground. Under sufficient load soil exhibits plastic deformation due to combination of permanent slip of soil particles relative to one another. In any type of soil, when shearing stress subjected, the soil grains tend to rearrange into a more dense packing results decrease in volume, less space in voids and water in pore spaces is forced out [2]. If drainage of pore water is impeded, pore water pressures increase progressively with the shear load. This leads to transfer of stress from the soil skeleton to the pore water precipitating a decrease in effective stress and shear resistance of soil. If the shear resistance of the soil becomes less than the static, driving shear stress, the soil can undergo large deformations and is said to liquefy [3]. As the bearing capacity of soil to sustain foundation load is directly related to strength, liquefaction poses a serious hazard to structures and must be assessed in areas where liquefaction prone deposit exist [4]. Eight types of failure commonly associated with soil liquefaction in earthquakes are

- Buoyant rise of buried structures such as tanks.
- Failure of retaining walls due to increased lateral loads from liquefied backfill soil or loss of support from liquefied foundation soils.
- Flow failures of slopes involving very large down-slope movements of a soil mass.
- Ground oscillation where liquefaction of a soil deposit beneath a level site leads to back and forth movements of intact blocks of surface soil.
- Ground settlement, often associated with some other failure mechanism.
- Lateral spreads resulting from the lateral displacement of gently sloping ground.
- Loss of bearing capacity causing foundations failures.
- Sand boils, occur when water under pressure wells up through a bed of sand.

Generally, highly sensitive clays lose the strength substantially during earthquake excitation. Fine and uniform sands are more prone to liquefaction, as the pore pressure is dissipated more quickly in coarse sand; hence the chances of liquefaction are reduced in coarse sand deposits [5].

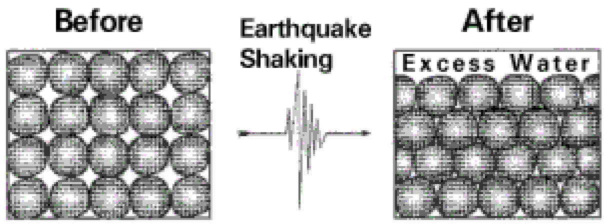

Fig. 1: pore water dissipated more quickly in sand

Due to the cost and the difficulty in acquiring undisturbed samples for analyses of liquefaction potential many empirical method based on in situ tests were developed, these are modified Seed's, Tokimatsu and Yoshimi (T-Y), Idriss and Boulanger (I-B) and new Japan Road Association (NJRA) methods etc. In these empirical methods I-B method is updated and modified version of simplified procedure so here we used I-B method. Field test data including the standard penetration test (SPT) have been used to develop liquefaction potential of soil by empirical method.

Now days a new technique called computational methods is being used frequently for the assessment of liquefaction potential as well as for the solution of various other engineering problems. Artificial neural network approach is one of them found suitable in the field of liquefaction potential assessment by various researchers like Goh, (1994); Goh, (1996); Wang and Rahman, 1999; Goh, (2002); Baziar and Nilipour, (2003); Neaupane and Achet, (2004); Baziar and Gharbani, (2005); Das and Basudhar, (2006); Hsu et al., (2006); Young-Su and Byung-Tak, (2006); Hanna et al., (2007); Rao and Satyam, (2007); Ramakrishnan et al., (2008); Farookhzad et al., (2010); Moradi et al., (2011) [6-13, 1, 14-17, 2, 18].

Current research is the effort of assessing liquefaction potential at the banks of river Ganga and Yamuna since alluvial soil is abundantly present in said areas. Soil strata on the bank of river Ganga and Yamuna mainly consists sandy and clayey soil at various depths. The upper part of strata contains major portion of silty soil and sandy silt enhancing probability. So there is a major chance of liquefaction occurrence in the upper soil zone at greater earthquake magnitude. Two different methods namely Idriss and Boulanger (I & B) and artificial neural network (ANN) modeling approach are used to find out liquefaction potential of soil. The developed ANN model could predict the liquefaction potential of soil.

1.1 Idriss and Boulanger method:

Geotechnical professionals generally investigate subsurface to evaluate the potential for liquefaction. The most common techniques using standard penetration test (SPT) blow count (commonly referred as to the "N-value") follows certain protocols:

1. Estimation of the cyclic stress ratio (CSR) induced at various depths within the soil by the earthquake.
2. Estimation of the cyclic resistance ratio (CRR) of the soil, i.e. the cyclic shear stress ratio which is required to cause initial liquefaction of the soil.
3. Evaluation of factor of safety against liquefaction potential of in situ soils

Calculation of CSR:

Modus operandi by Idriss & Boulanger [20] for evaluation of CSR is same as "simplified method". Right after CSR calculated from the eqn.

$$\mathrm{CSR} = {}^{\tau_{avg}}/_{\sigma'_v} = 0.65\left({}^{a_{max}}/_{g}\right)\left({}^{\sigma_v}/_{\sigma'_v}\right)\mathrm{r_d} \qquad (1)$$

Value of CSR is adjusted for the moment magnitude M = 7.5. Accordingly the value of CSR is given as

$$(CSR)_{M=7.5} = {}^{CSR}/_{MSF} = 0.65\left({}^{\sigma_v a_{max}}/_{\sigma'_v}\right)\frac{r_d}{MSF} \qquad (2)$$

A new parameter r_d which could be adequately expressed as a function of depth and earthquake magnitude (M) was introduced and may be explain from following relations:

$$\ln(r_d) = \propto(z) + \beta(z)M \qquad (3)$$

$$\propto(z) = -1.012 - 1.126\sin\left({}^{z}/_{11.73} + 5.133\right) \qquad (4a)$$

$$\beta(z) = 0.106 + 0.118\sin\left({}^{z}/_{11.28} + 5.142\right) \qquad (4b)$$

Where z is the depth in meters and M is moment magnitude. These equations were appropriated for depth z ≤ 34 m however for depth z > 34m; the following expression may be used:

$$\mathrm{r_d} = 0.12\exp(0.22M) \qquad (5)$$

$CSR_{7.5}$ is the cyclic stress ratio for magnitude of 7.5 earthquakes, magnitude smaller or larger than 7.5, introduces a correction factor namely magnitude scaling factor MSF defined by the following equation given by [20]:

$$\mathrm{MSF} = {}^{10^{2.24}}/_{M^{2.56}} \qquad (6)$$

Calculation of CRR:

Idriss and Boulanger [21] adjusted the equation of CRR for clean sands as follows

$$CRR = \exp\left\{\frac{(N_1)_{60cs}}{14.1} + \left(\frac{(N_1)_{60cs}}{126}\right)^2 - \left(\frac{(N_1)_{60cs}}{23.6}\right)^3 + \left(\frac{(N_1)_{60cs}}{25.4}\right)^4 - 2.8\right\} \quad (7)$$

Subsequent expressions describes the way parameters in the above equation is calculated

$$(N_1)_{60cs} = (N_1)_{60} + (\Delta N_1)_{60} \quad (8a)$$

$$(\Delta N_1)_{60} = exp\left(1.63 + {}^{9.7}/_{FC} - \left({}^{15.7}/_{FC}\right)\right) \quad (8b)$$

$$(N_1)_{60} = C_N (N)_{60} \quad (8c)$$

The variation of $(\Delta N_1)_{60}$ with FC, calculated using the eqn. (8c) is presented in fig. 2.

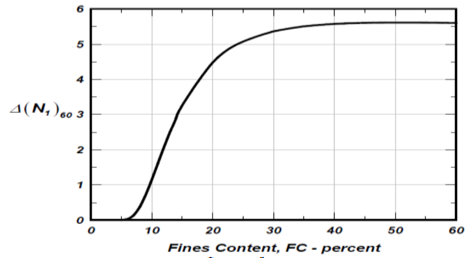

Fig. 2 Variation of $(\Delta N_1)_{60}$ with fines content

The use of equations in preceding articles provides a convenient means for evaluating the cyclic stress ratio required to cause liquefaction for cohesion-less soils with varying fines content.

Calculation of factor of safety:

If the cyclic stress ratio caused by an earthquake is greater than the cyclic resistance ratio of the in situ soil, then liquefaction could occur during the earthquake, and vice versa. The factor of safety (FOS) against liquefaction is defined as:

$$FS_{Liquefaction} = {}^{CRR}/_{CSR} \quad (9)$$

Liquefaction is predicted to occur when FS≤ 1.0, and liquefaction predicted not to occur when FS > 1. The higher the factor of safety, the more resistant against liquefaction [22], however, soil that has a factor of safety slightly higher than 1.0 may still liquefy during the earthquake.

1.2 Overview of Artificial Neural Network:

Artificial neural network (ANN) consists of a large number of interconnected processing units known as biological neuron [9]. It is a soft computing approach that is inspired by the function and structural aspects of biological neurons. ANN is advanced and standard tools simulated by the mathematical model and computational model of the human brain and being used around the globe to find solutions to a wide variety of non-linear statistical data complications [15]. They are usually used to model complex relationship among inputs and targets to find patterns in datasets. Interconnections among neurons are established by weights, which are applied to all values passing through one neuron to another. The ANNs are arranged in three or more layers, one input layer, one or more hidden layers and one target layer. Each layer of neurons has connections to all the neurons in next layer. Each neuron receives an input signals from the previous neurons connected. Each of these connections has numeric weights associated with it.

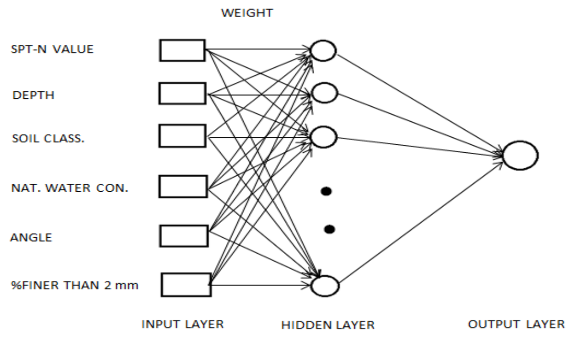

Fig. 3: A two-layer feed-forward artificial neural network structure.

The signals from each input are then processed through a weighted sum of the inputs, and the processed output signal is then transmitted another neuron via a transfer of activation function. Once the network trained with sufficient number of datasets, it can validate, the trained network required to make predictions for a new set of data that it has never been introduced during the previous phases [17]. Due to its multidisciplinary nature, ANN is becoming advanced and standard tool for accomplishment of their work. ANN model have also been used in the field of geotechnical engineering. A two layer feed-forward ANN structure is shown above in fig. 3.

Feed-forward back propagation technique:

In this section here we used Feed-forward back propagation technique. In this technique learning algorithm has two stages. In first stage, the inputs are forwarded from input layer to output layer. After computing the errors of each output between computed and desired output, in second stage information is send backward to the inputs which readjust the connecting weights in the hidden and output layer to minimize this error. The modification of the weights is carried out by using generalized delta rule [23].

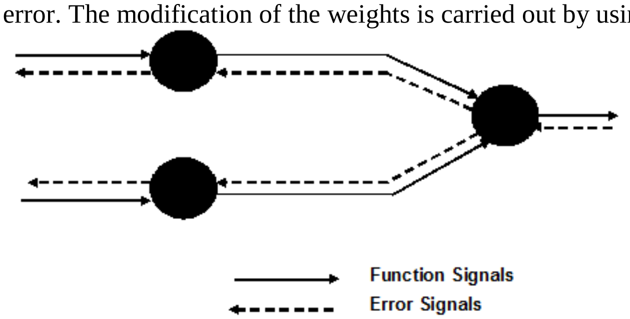

Fig. 4: Feed-forward back propagation network

Activation/Transfer function:

Though many activation functions exist, the most common is the sigmoid activation function, which outputs a number between 0 (for low input values) and 1 (for high input values). The resultant of this function is then passed as the input to other neurons through more connections, each of which are weighted [24]. Sigmoid transfer function is expressed as:

$$f(t) = \frac{1}{1+\exp(-t)} \quad (10)$$

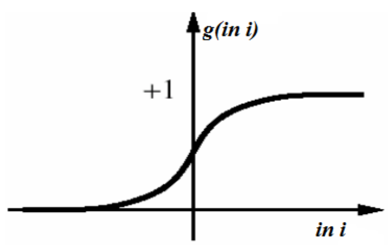

Fig. 5: Sigmoid transfer function.

2. Development of ANN models:

To estimate liquefaction potential of sandy soil SPT tests on different stations were conducted as it is the most suitable site exploration test for sandy soil. Data collected from SPT tests were utilized to find out liquefaction potential through I & B method, further these data were used to develop ANN models. Output parameter that is occurrence of liquefaction in the ANN model is designed to answer in yes/no format based on I & B method. The soil properties found through SPT and other laboratory tests used as input vectors in ANN method is shown in table 1. The detailed methodology adopted is discussed under following sub-headings.

2.1 Experimental method:

Standard penetration test were conducted in order to collect bore-hole datasets. Disturbed and undisturbed soil specimen was collected from these bore-holes up to depth of 10 meters as well as SPT N-values were also determined at a regular interval of depth 1.5 m, disturbed soil samples were used to determine liquid limit; plastic limit; angle of internal friction; particle size finer than 2 mm, 0.075 mm and 0.002mm and undisturbed samples were used to find out natural water content, bulk unit weight. All experiments were conducted according to bureau of Indian standard's guidelines for soil testing.

Data modification:

Corrected SPT-N values were required to apply I & B method to calculate liquefaction potential hence standard method for SPT-N value correction was adopted as given by IS: 2131-1981. A brief discussion on corrected SPT-N value is discussed hereunder:

Correction for overburden pressure: N- value obtained from SPT test is corrected first which is either calculated by the equation:

$$N_1=C_N \times N \qquad (11)$$

C_N is correction factor obtained directly from the graph given in Indian Standard Code (IS: 3121-1981). (Fig. 6)

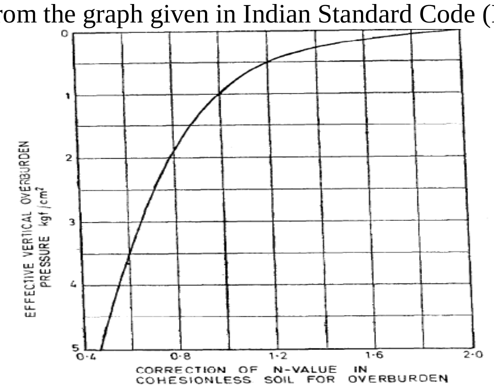

Fig. 6: Correction due to overburden pressure

It can also calculate from the formulae:

$$C_N=0.77\log_{10}\frac{2000}{p} \qquad (12)$$

Where, p is effective overburden pressure in kN/m^2 [25].

Dilatancy correction: The values obtained in overburden pressure (N_1) shall be corrected for dilatancy if the stratum consist of fine sand and silt below water table for values of N_1 greater than 15 as under [26]:

$$N_c = 15 + 0.5(N_1 -15) \qquad (13)$$

Calculation of CSR value through I & B method is calculated for specific depth of water table and earthquake magnitude. Therefore CSR values were interpreted for different combination of depth and earthquake magnitude as shown below in table 1.

2.2 Network Architecture:

A total combination of 6 input variables comprising depth (z), SPT-N value (N), classification of soil, natural / field moisture content (w), angle of internal friction (φ) and particle size finer than 2 mm were used for ANN model development. Soil classification criteria were implemented by encoding soil class with a specific value keeping in view sand content in respective soil specimen. Table 3 illustrates soil encoding for different soil class [9]. A total of 160 datasets were used for training in which 27 datasets were reserved for validating the network. The boundaries for input and output parameters of the models are listed in Table 2. The input–output data of each ANN model were scaled to lie between 0 and 1 by using Eqn. (14).

$$\alpha=\frac{\alpha_{actual}-\alpha_{min}}{\alpha_{max}-\alpha_{min}} \qquad (14)$$

Where α_{norm} is the normalized value, α is the actual value, α_{max} is the maximum value and α_{min} is the minimum value.

ANN tool built in MATLAB (R2011a) software was used for all operations in which networks were trained with single or double hidden layers of varying numbers of neurons (2 to 20) were used in the analysis. Fig. 3 describes the way network were treated from given set of input and target parameters.

To identify its fundamental attributes a coding method was used for different depth of water table and earthquake magnitude, as such W_XM_Y denotes W_X: depth of water table and M_Y: earthquake magnitude value. For each and every set of depth of water table and earthquake magnitude, we build different number of ANN architecture with varying hidden layer and number of neurons in each hidden layer. In this thesis, here we choose one and two hidden layers and neurons in hidden layer is varied up to 20. ANN architecture is simply denoted as N_X, which is varied from N_1 to N_{52}. Some of the liquefaction values obtained through selected ANN architecture for each network are discussed in subsequent literature.

3. Results and Discussion:

As mentioned above three water table depth and three earthquake magnitude values were considered for assessing liquefaction potential through I & B and ANN method. This resulted in total of nine set of liquefaction values through nine combinations of water table and earthquake magnitude values. Table 4-6 shows that liquefaction potential evaluated from I & B method and computed by ANN models for the datasets which are reserved for validating. Calculation of errors between liquefaction potential by I & B method and ANN model is also shown in table 4-6.

Using the liquefaction values through I & B method and ANN (by validating the networks) method, graphs (fig. no. 6-14) were prepared for comparative analysis for these nine set of combinations of depth of water table and earthquake magnitude values however input vectors retained common in all ANN models (i.e. 6 number of inputs). For each nine set, we trained the network throughout the ANN architecture with varying epochs from 500 to 5000. Weights were randomly initialized. The numbers of hidden neurons are varied (4, 6, 8..... 20) and the generalization performance is reported in Table 2. Here we select four number of ANN architecture for each set those mean square error (MSE) is low and regression is high. After that, we calculate average absolute error for the selected ANN architecture and finally one model is selected on the basis of minimum average absolute error and high regression value. Absolute average error calculated for nine models is summarized in table no. 7.

From the graph, here we see that regression for validation is varied from 0.967 to 0.9969 and average absolute error is varied from 0.929% to 2.687%. An illustration of regression graph for network N_{21} is also shown in fig. 15. Moreover results obtained in occurrence/non-occurrence form of liquefaction for particular combination of depth of water table and earthquake magnitude values are as shown in table no. 4-6 for ANN method indicates closeness of predicted value to I & B method. In some cases like $W_3M_{7.5}$ serial no. 6, $W_4M_{7.5}$ serial no. 5 and 6, W_5M_7 serial no. 3, $W_5M_{7.5}$ serial no. 6 and W_5M_8 serial no. 13 are wrongly predicted by the respective model because of the ratio of CRR/ CSR is nearly equal to 1 .

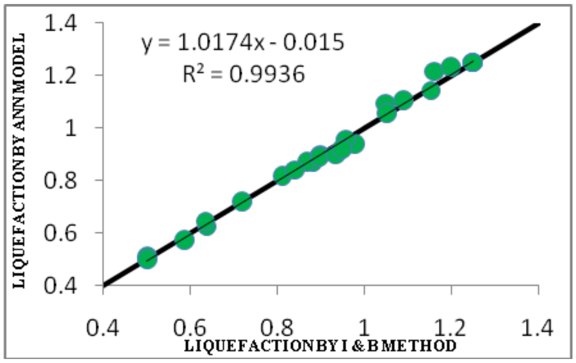

Fig. 6: Comparison study for W.T. 3m and M 7

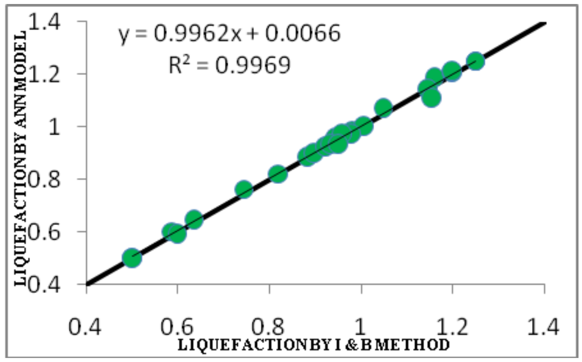

Fig. 9: Comparison study for W.T. 4m and M 7

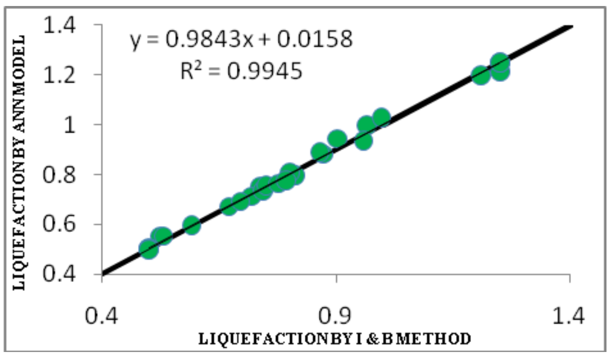

Fig. 7: Comparison study for W.T. 3m and M 7.5

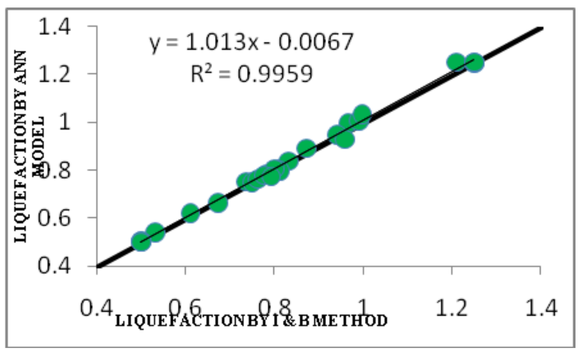

Fig. 10: Comparison study for W.T. 4m and M 7.5

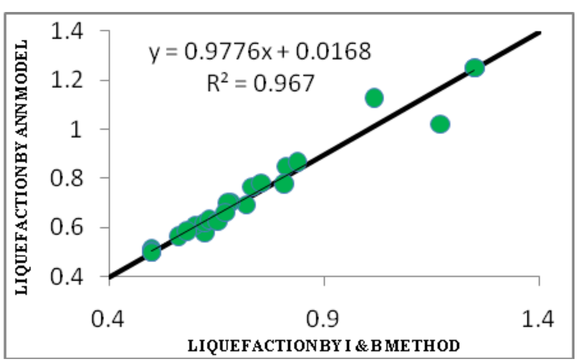

Fig. 8: Comparison study for W.T. 3m and M 8

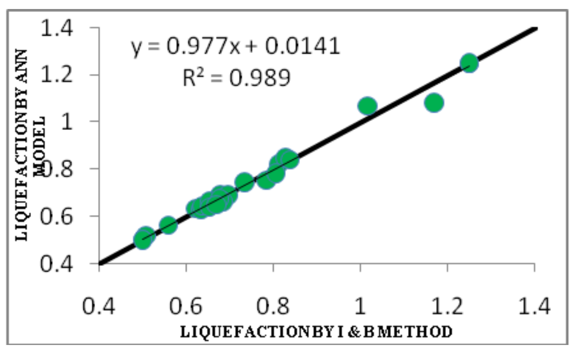

Fig. 11: Comparison study for W.T. 4m and M 8

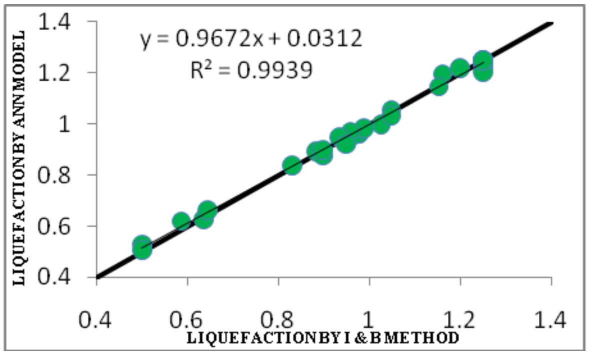

Fig. 12: Comparison study for W.T. 5m and M 7

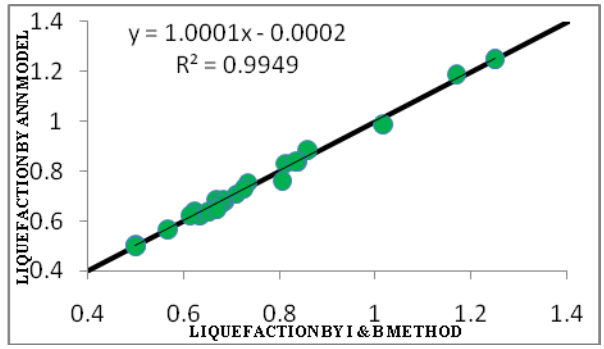

Fig. 14: Comparison study for W.T. 5m and M 8

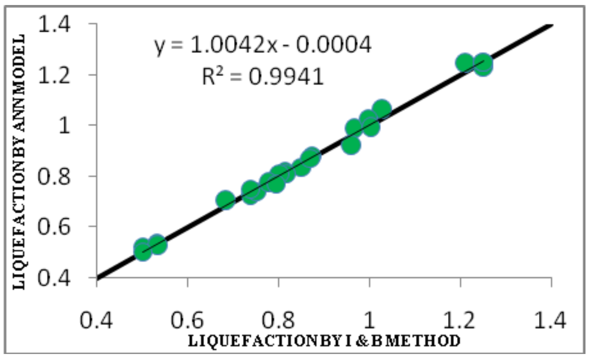

Fig. 13: Comparison study for W.T. 5m and M 7.5

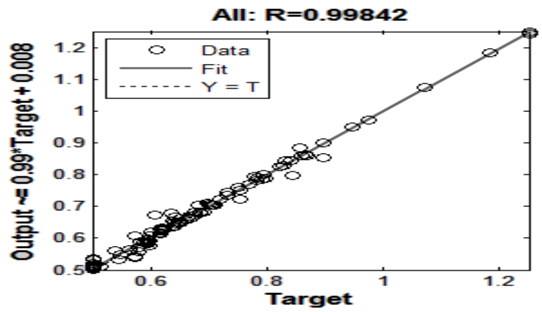

Fig. 15: Overall regression for Network N_{21}

4. Conclusions:

Artificial neural network have been developed for the assessment of liquefaction potential with field and laboratory datasets. This paper has established the usefulness of the ANN to model the complex relationship between the soil, seismic parameters and the liquefaction potential using in situ measurements based on SPT test. Coefficient of correlation values in all models are greater than 0.96 indicate satisfactory prediction capability of ANN models. Moreover, results obtained in occurrence/non-occurrence form of liquefaction for particular combination of depth of water table and earthquake magnitude values by ANN method indicates closer predictions compared to I & B method.

Field and Lab input parameters may directly be used as input vector for ANN models, which is simpler than the conventional methods to predict Liquefaction Potential. The prediction using ANN with SPT data had an overall success rate of ninety six percent resulting very effective and easily handle tool.

References:

[1]. S. Hsu, M. Yang, M. Chen, and J. Lin, Artificial Neural Network of liquefaction evaluation for soils with High Fines Content, 2006 international joint conference on neural networks, Canada. July 16-21 (2006) pp2643-2649.

[2]. F. Farrokhzad, A.J. Choobasti, and A. Barari, Liquefaction microzonation of Babool city using artificial neural network, 2010 Journal of king saud university (science) (2010).

[3]. H.B. Seed and I. M. Idriss, Summer Report on Ground Motions and Soil Liquefaction during Earthquakes, 1982 Earthquake Engineering Research Institute, Berkeley, California (1982).

[4]. Prasad, B.B., Fundamentals of soil dynamics and earthquake engineering by, PHI learning private limited, new delhi-110001, 2009.

[5]. Haykin, S., Neural Networks: A Comprehensive Foundation, 2nd edition, Prentice-Hall, Englewood Cliffs, NJ 1998.

[6]. A.T.C. Goh, Seismic liquefaction potential assessed by neural networks, 1994, *Journal of Geotechnical Engineering,* Vol. 120, No. 9, September, 1994, pp1467-1480.

[7]. A.T.C. Goh, Pile driving records reanalyzed using neural networks, J Geotech Engrg, ASCE 1996; 122(6) pp492–500.

[8]. J. Wang, and M.S. Rahman, A neural network model for liquefaction-induced horizontal ground displacement, 1999, Soil Dynamics and Earthquake Engineering. 18 (1999) pp555–568.

[9]. A.T.C. Goh, Probabilistic neural network for evaluating seismic liquefaction potential, 2002, Can. Geotech. J. (39) pp.219-232.

[10]. M.H. Baziar, N. Nilipour, Evaluation of liquefaction potential using neural-networks and CPT results, 2003, Soil Dynamics and Earthquake Engineering 23 (2003) pp631–636.

[11]. K.M. Neaupane, S.H. Achet, Use of backpropagation neural network for landslide monitoring: a case study in the higher Himalaya, 2004, Engineering Geology 74 (2004) pp213–226.

[12]. M.H. Baziar, A. Ghorbani, Evaluation of lateral spreading using artificial neural networks, 2005, Soil Dynamics and Earthquake Engineering 25 (2005) pp1–9.

[13]. S.K. Das, P.K. Basudhar, Undrained lateral load capacity of piles in clay using artificial neural network, 2006, Computers and Geotechnics 33 (2006) pp454–459.

[14]. K. Young-Su, and K. Byung-Tak, Use of Artificial Neural Networks in the Prediction of Liquefaction Resistance of Sands, 2006, Journal of Geotechnical and Geo-environmental Engineering ASCE (2006) pp1502-1504.

[15]. A.M. Hanna, D. Ural, and G. Saygili, Neural network model for liquefaction potential in soil deposits using Turkey and Taiwan earthquake data, 2007, Soil Dynamics and Earthquake Engineering 27 (2007a) pp521–540.

[16]. A.M. Hanna, D. Ural, and G. Saygili, Evaluation of liquefaction potential of soil deposits using artificial neural networks, 2007, International journal for computer-aided engineering and software, 24(1) (2007b) pp5-16.

[17]. K.S. Rao and D.N. Satyam, Liquefaction studies for seismic microzonation of Delhi region, 2007, Current science, vol. 92, no. 5 (10 march 2007), pp646-654.

[18]. D. Ramakrishnan, T.N. Singh, N. Purwar, K.S. Barde, Akshay, Gulati and S. Gupta, Artificial neural network and liquefaction susceptibility assessment: a case study using the 2001 Bhuj earthquake data, Gujarat, India, 2008, Comput Geosci (2008) 12: pp491-501.

[19]. G. Moradi, B.R. Khatiba, and M.H. Sutubadi, Determination of liquefaction potential of soil using $(N_1)_{60}$ by numerical modeling method, 2011, EJGE, vol. 16 (2011) pp407-417.

[20]. I.M. Idriss, and R.W. Boulanger, Semi-empirical procedures for evaluating liquefaction potential during earthquakes, 2006, Soil Dynamics and Earthquake Engineering. 26 (2006) pp115-130.

[21]. T. L. Youd, and I. M. Idriss, NCEER Workshop on Evaluation of Liquefaction Resistance of Soils, 1997, Nat. Ctr. for Earthquake Engg. Res., State Univ. of New York at Buffalo eds. (1997).

[22]. Youd et al., Liquefaction resistance of soils: summary report from the 1996 NCEER and 1998 NCEER/NSF workshops on evaluation of liquefaction resistance of soils, 2001, J. Geotech. Engg. Div.. ASCE, 127(10) (2001) pp817-833.

[23]. D.E. Rumelhart, G.E. Hinton, and R.J. Williams, “Learning Internal Representations by Error Propagation”. In David E. Rumelhart, James L. McClelland, and the PDP Research Group, editors, Parallel Distributed Processing. Explorations in the Microstructure of Cognition, 1986, MIT Press, Volume 1: Foundations, pp318-364.

[24]. Krose, B. and Smagt, P.V.D., An introduction to neural networks, University of Amsterdam, Eighth edition, Nov-1996.

[25]. Terzaghi K., Peck R. B., and Mesri G., Soil mechanics in engineering practice (2nd Ed.), Wiley & Sons Inc., New York 1996.

[26]. Varghese, P.C. Foundation Engineering, prentice hall of India private limited, New Delhi – 110001, 2007.

Illustrations:

Table 1: Assumed water table and earthquake magnitude.

Depth of water table (m)	3	4	5
Earthquake magnitude (rector scale)	7.0	7.5	8.0

Table 2: Range of input and output parameters.

Input Parameters	**minimum**	**maximum**
depth (m)	0	10
SPT-N value	0	50
Soil classification	0	5
Natural water content	0.55	32.36
Angle of internal friction	12	33
Particle finer than 2 mm (%)	82.5	100
Liquefaction potential	0.5	1.25

Table 3: Soil class with respective number.

Soil description	**Soil type number**
Poorly graded sand (SP)	5
Silty sand (SM)	4
Very fine sand (ML)	3
Silty clay with low plasticity (CL)	2
Sandy clay with medium plasticity (CI)	1

Table 4: Comparison study about liquefaction potential for water table at 3m.

S. No.	Depth (z)	SPT-N value	**For network W_3M_7**				**For network $W_3M_{7.5}$**				**For network W_3M_8**			
			Lique. Pot. by I & B method		Lique. Pot. by ANN		Lique. Pot. by I & B method		Lique. Pot. by ANN		Lique. Pot. by I&B method		Lique. Pot. by ANN	
			ratio	status	ratio	status	ratio	status	ratio	status	ratio	status	ratio	status
1	1.5	12	0.882	Yes	0.873	Yes	0.737	Yes	0.753	Yes	0.737	Yes	0.579	Yes
2	3.0	22	1.161	No	1.215	No	0.966	Yes	0.996	Yes	0.966	Yes	0.848	Yes
3	4.5	20	0.868	Yes	0.87	Yes	0.718	Yes	0.713	Yes	0.718	Yes	0.609	Yes
4	3.0	19	1.049	No	1.095	No	0.873	Yes	0.882	Yes	0.873	Yes	0.766	Yes
5	4.5	26	1.09	No	1.106	No	0.902	Yes	0.943	Yes	0.902	Yes	0.78	Yes
6	3.0	23	1.199	No	1.234	No	0.997	Yes	1.028	No	0.997	Yes	0.867	Yes
7	4.5	21	0.899	Yes	0.898	Yes	0.744	Yes	0.735	Yes	0.744	Yes	0.62	Yes
8	6.0	29	1.052	No	1.056	No	0.865	Yes	0.889	Yes	0.865	Yes	0.692	Yes
9	1.5	12	0.897	Yes	0.891	Yes	0.75	Yes	0.755	Yes	0.75	Yes	0.633	Yes
10	3.0	16	0.978	Yes	0.939	Yes	0.814	Yes	0.796	Yes	0.814	Yes	0.702	Yes
11	4.5	18	0.811	Yes	0.816	Yes	0.671	Yes	0.671	Yes	0.671	Yes	0.563	Yes
12	6.0	16	0.638	Yes	0.625	Yes	0.525	Yes	0.552	Yes	0.525	Yes	0.501	Yes
13	3.0	28	1.25	No	1.25	No	1.209	No	1.199	No	1.209	No	1.128	No
14	4.5	19	0.84	Yes	0.84	Yes	0.695	Yes	0.691	Yes	0.695	Yes	0.584	Yes
15	6.0	19	0.719	Yes	0.721	Yes	0.591	Yes	0.597	Yes	0.591	Yes	0.51	Yes
16	1.5	25	1.25	No	1.25	No	1.25	No	1.214	No	1.25	No	1.022	No
17	3.0	50	1.25	No	1.25	No	1.25	No	1.25	No	1.25	No	1.25	No
18	1.5	14	0.958	Yes	0.958	Yes	0.801	Yes	0.806	Yes	0.801	Yes	0.701	Yes
19	3.0	16	0.933	Yes	0.899	Yes	0.777	Yes	0.763	Yes	0.777	Yes	0.625	Yes
20	1.5	13	0.949	Yes	0.921	Yes	0.793	Yes	0.777	Yes	0.793	Yes	0.661	Yes
21	3.0	20	1.153	No	1.143	No	0.959	Yes	0.935	Yes	0.959	Yes	0.779	Yes
22	4.5	50	1.25	No	1.25	No	1.25	No	1.25	No	1.25	No	1.25	No
23	1.5	7	0.635	Yes	0.645	Yes	0.531	Yes	0.552	Yes	0.531	Yes	0.511	Yes
24	3.0	7	0.587	Yes	0.574	Yes	0.5	Yes	0.507	Yes	0.5	Yes	0.501	Yes
25	4.5	8	0.5	Yes	0.508	Yes	0.5	Yes	0.501	Yes	0.5	Yes	0.5	Yes
26	7.5	5	0.5	Yes	0.501	Yes	0.5	Yes	0.5	Yes	0.5	Yes	0.5	Yes
27	9.0	5	0.5	Yes	0.5	Yes	0.5	Yes	0.5	Yes	0.5	Yes	0.5	Yes

Table 5: Comparison study about liquefaction potential for water table at 4m.

S. No.	Depth (z)	SPT-N value	**For network W_4M_7**				**For network $W_4M_{7.5}$**				**For network W_4M_8**			
			Lique. Pot. by I & B method		Lique. Pot. by ANN		Lique. Pot. by I & B method		Lique. Pot. by ANN		Lique. Pot. by I & B method		Lique. Pot. by ANN	
			ratio	status	ratio	status	ratio	status	ratio	status	ratio	status	ratio	status
1	1.5	12	0.882	Yes	0.887	Yes	0.737	Yes	0.752	Yes	0.623	Yes	0.633	Yes
2	3.0	22	1.161	No	1.187	No	0.966	Yes	0.996	Yes	0.812	Yes	0.82	Yes
3	4.5	20	0.98	Yes	0.983	Yes	0.811	Yes	0.805	Yes	0.678	Yes	0.689	Yes
4	3.0	19	1.049	No	1.071	No	0.873	Yes	0.892	Yes	0.734	Yes	0.743	Yes
5	4.5	26	1.197	No	1.207	No	0.991	Yes	1.008	No	0.829	Yes	0.847	Yes
6	3.0	23	1.199	No	1.213	No	0.997	Yes	1.032	No	0.839	Yes	0.839	Yes
7	4.5	21	1.006	No	1.002	No	0.832	Yes	0.838	Yes	0.696	Yes	0.691	Yes
8	6.0	29	1.146	No	1.143	No	0.942	Yes	0.947	Yes	0.783	Yes	0.753	Yes
9	1.5	12	0.897	Yes	0.9	Yes	0.75	Yes	0.749	Yes	0.634	Yes	0.63	Yes
10	3.0	16	0.978	Yes	0.974	Yes	0.814	Yes	0.796	Yes	0.684	Yes	0.662	Yes
11	4.5	18	0.921	Yes	0.925	Yes	0.762	Yes	0.763	Yes	0.637	Yes	0.644	Yes
12	6.0	16	0.744	Yes	0.76	Yes	0.612	Yes	0.619	Yes	0.509	Yes	0.518	Yes
13	3.0	28	1.25	No	1.25	No	1.209	No	1.249	No	1.017	No	1.068	No
14	4.5	19	0.945	Yes	0.958	Yes	0.782	Yes	0.783	Yes	0.654	Yes	0.665	Yes
15	6.0	19	0.818	Yes	0.82	Yes	0.672	Yes	0.663	Yes	0.559	Yes	0.563	Yes
16	1.5	25	1.25	No	1.25	No	1.25	No	1.245	No	1.17	No	1.081	No
17	3.0	50	1.25	No	1.25	No	1.25	No	1.25	No	1.25	No	1.248	No
18	1.5	14	0.958	Yes	0.973	Yes	0.801	Yes	0.806	Yes	0.677	Yes	0.673	Yes
19	3.0	16	0.933	Yes	0.934	Yes	0.777	Yes	0.778	Yes	0.653	Yes	0.638	Yes
20	1.5	13	0.949	Yes	0.934	Yes	0.793	Yes	0.774	Yes	0.67	Yes	0.65	Yes
21	3.0	20	1.153	No	1.109	No	0.959	Yes	0.929	Yes	0.807	Yes	0.781	Yes
22	4.5	50	1.25	No	1.25	No	1.25	No	1.25	No	1.25	No	1.25	No
23	1.5	7	0.635	Yes	0.645	Yes	0.531	Yes	0.539	Yes	0.5	Yes	0.502	Yes
24	3.0	7	0.587	Yes	0.599	Yes	0.5	Yes	0.506	Yes	0.5	Yes	0.5	Yes
25	4.5	8	0.6	Yes	0.592	Yes	0.5	Yes	0.501	Yes	0.5	Yes	0.5	Yes
26	7.5	5	0.5	Yes	0.501	Yes	0.5	Yes	0.5	Yes	0.5	Yes	0.5	Yes
27	9.0	5	0.5	Yes	0.5	Yes	0.5	Yes	0.5	Yes	0.5	Yes	0.5	Yes

Table 6: Comparison study about liquefaction potential for water table at 5m.

S. No.	Depth (z)	SPT-N value	For network W_5M_7				For network $W_5M_{7.5}$				For network W_5M_8			
			Lique. Pot. by I & B method		Lique. Pot. by ANN		Lique. Pot. by I & B method		Lique. Pot. by ANN		Lique. Pot. by I & B method		Lique. Pot. by ANN	
			ratio	status	ratio	status	ratio	status	ratio	status	ratio	status	ratio	status
1	1.5	12	0.882	Yes	0.892	Yes	0.737	Yes	0.727	Yes	0.608	Yes	0.637	Yes
2	3.0	22	1.161	No	1.195	No	0.966	Yes	0.989	Yes	0.832	Yes	0.83	Yes
3	4.5	20	1.025	No	0.999	Yes	0.849	Yes	0.835	Yes	0.702	Yes	0.707	Yes
4	3.0	19	1.049	No	1.056	No	0.873	Yes	0.88	Yes	0.743	Yes	0.753	Yes
5	4.5	26	1.25	No	1.225	No	1.027	No	1.065	No	0.857	Yes	0.884	Yes
6	3.0	23	1.199	No	1.218	No	0.997	Yes	1.027	No	0.856	Yes	0.84	Yes
7	4.5	21	1.049	No	1.032	No	0.868	Yes	0.87	Yes	0.724	Yes	0.731	Yes
8	6.0	29	1.25	No	1.202	No	1.003	No	0.995	No	0.803	Yes	0.837	Yes
9	1.5	12	0.897	Yes	0.875	Yes	0.75	Yes	0.74	Yes	0.635	Yes	0.619	Yes
10	3.0	16	0.978	Yes	0.964	Yes	0.814	Yes	0.817	Yes	0.653	Yes	0.676	Yes
11	4.5	18	0.966	Yes	0.955	Yes	0.799	Yes	0.803	Yes	0.666	Yes	0.687	Yes
12	6.0	16	0.829	Yes	0.836	Yes	0.682	Yes	0.705	Yes	0.575	Yes	0.567	Yes
13	3.0	28	1.25	No	1.249	No	1.209	No	1.247	No	1.084	No	0.988	Yes
14	4.5	19	0.987	Yes	0.983	Yes	0.817	Yes	0.81	Yes	0.688	Yes	0.684	Yes
15	6.0	19	0.897	Yes	0.899	Yes	0.738	Yes	0.749	Yes	0.627	Yes	0.623	Yes
16	1.5	25	1.25	No	1.249	No	1.25	No	1.233	No	1.074	No	1.187	No
17	3.0	50	1.25	No	1.25	No	1.25	No	1.25	No	1.25	No	1.25	No
18	1.5	14	0.958	Yes	0.971	Yes	0.801	Yes	0.809	Yes	0.697	Yes	0.669	Yes
19	3.0	16	0.933	Yes	0.949	Yes	0.777	Yes	0.778	Yes	0.65	Yes	0.639	Yes
20	1.5	13	0.949	Yes	0.921	Yes	0.793	Yes	0.769	Yes	0.657	Yes	0.649	Yes
21	3.0	20	1.153	No	1.145	No	0.959	Yes	0.922	Yes	0.795	Yes	0.762	Yes
22	4.5	50	1.25	No	1.25	No	1.25	No	1.25	No	1.25	No	1.25	No
23	1.5	7	0.635	Yes	0.628	Yes	0.531	Yes	0.533	Yes	0.511	Yes	0.504	Yes
24	3.0	7	0.587	Yes	0.619	Yes	0.5	Yes	0.521	Yes	0.505	Yes	0.501	Yes
25	4.5	8	0.644	Yes	0.661	Yes	0.533	Yes	0.529	Yes	0.504	Yes	0.501	Yes
26	7.5	5	0.5	Yes	0.53	Yes	0.5	Yes	0.502	Yes	0.5	Yes	0.5	Yes
27	9.0	5	0.5	Yes	0.507	Yes	0.5	Yes	0.502	Yes	0.5	Yes	0.5	Yes

Table 7: Details of errors and architecture for one of the best model.

model no.	W_3M_7	$W_3M_{7.5}$	W_3M_8	W_4M_7	$W_4M_{7.5}$	W_4M_8	W_5M_7	$W_5M_{7.5}$	W_5M_8
Network Name	N_{10}	N_2	N_4	N_{10}	N_{10}	N_{10}	N_{19}	N_{19}	N_{21}
Network Architecture	6-6-2-1	6-6-1	6-10-1	6-6-2-1	6-6-2-1	6-6-2-1	6-12-2-1	6-12-2-1	6-12-6-1
Avg. Abs. Error (%)	1.337	1.645	2.687	0.929	1.207	1.625	1.713	1.513	1.382
MSE $\times 10^{-4}$	1.5155	1.0687	1.8804	1.9927	1.5585	0.4467	2.7934	1.5633	0.222
epoch	4000	5000	1000	4000	2000	2000	4000	3000	2000
Regression	0.99553	0.99852	0.99851	0.99029	0.99757	0.99818	0.99441	0.99791	0.99842
Coeff. of correlation	0.9936	0.9945	0.9670	0.9969	0.9959	0.9890	0.9939	0.9941	0.9949